

# Nonaqueous gold colloids. Investigations of deposition and film growth on organically modified substrates and trapping of molecular gold clusters with an alkyl amine†

Fei Tian and Kenneth J. Klabunde\*

Department of Chemistry, Willard Hall, Kansas State University, Manhattan, KS 66506, USA

Gold–acetone colloidal solutions were prepared by a metal vapor codeposition procedure (solvated metal atom dispersion) and from these solutions gold films were prepared by allowing adsorption/deposition on (sulfanylpropyl)trimethoxysilane- (aminopropyl)trimethoxysilane or (isobutyl)trimethoxysilane-modified substrates. The mechanism of gold film formation was studied by AFM and TEM. At short contact times, self-assembly of colloidal gold particles onto the functionalized substrate surfaces took place and both individual particles and aggregates appeared. As contact time increased, a dynamic equilibrium was evident on the thiol- and amine-modified substrates and resulted in the development of more stable, close-packed layers. At still longer contact times, a smooth film was formed on the surface. Besides film growth studies, the gold colloid particle growth in acetone was investigated. By adding dodecylamine, particle growth was stunted and very small (2–3 nm) individual crystallites coated by the amine were obtained. These materials were molecular in nature in the sense that they could be precipitated and redissolved many times without change. TEM data showed that the particles were spatially separated and the interparticle spacing was dependent on the amount of dodecylamine. The FT-IR data indicated that a significant amount of amine (N–H bond) and acetone (C=O bond) were adsorbed on the gold particle surfaces.

In recent years, aqueous gold colloids and films derived from them have undergone extensive study.<sup>1–6</sup> There are fewer studies dealing with nonaqueous colloids and derived films.<sup>7–9</sup> In aqueous colloidal solution, there are many counter ions, reduction byproducts or pyrolysis products present. However, in nonaqueous colloidal dispersions, only metal particles and pure solvent (and some adsorbed solvent fragments) are present and the colloidal solutions are free of interfering ions and impurities (chloride ion, *etc.*).

This difference results in a very important property for some metal–solvent combinations: particle growth to films can occur under very mild conditions and can be induced simply by solvent evaporation.<sup>10,11</sup> However, there are drawbacks to this approach. The biggest problem is that adhesion of the metal film to substrate surfaces is generally not good. Heat treatment can be used to increase the adhesion of films, but results are variable depending on the substrate materials.<sup>8b</sup>

Previous investigations of film growth from aqueous colloidal solutions have shown that gold particles strongly bind to substrate surfaces that have been derivatized with functional groups such as cyanide (–CN), amine (–NH<sub>2</sub>) or thiol (–SH), and in this way, well-defined single layers of gold particles have been laid down.<sup>3–6</sup>

Although nonaqueous gold colloids have been demonstrated to be good film precursors,<sup>8b,9</sup> controlled studies of film growth on well-defined derivatized surfaces have not been done. Herein we report such studies, which were undertaken as an attempt to better understand what controls deposition rates and to clarify mechanisms. Thus, we chose to study gold film growth on organically modified substrates [functional groups were thiol (–SH), amine (–NH<sub>2</sub>) and methyl (–CH<sub>3</sub>)], using colloidal suspensions of gold in acetone as a model (Au–acetone solutions were prepared by a metal vapor method reported earlier).<sup>7,10,12</sup> Furthermore, in related

research on the Au–acetone precursor solution, we have carried out some studies directed at trapping very small gold clusters during the atom aggregation process in cold acetone.

## Experimental

### Preparations

**Preparation of silane-modified glass substrates.** Glass microscope slides (3 × 1.5 × 0.2 cm) were cleaned in 1 : 4 30% H<sub>2</sub>O<sub>2</sub> : 98% H<sub>2</sub>SO<sub>4</sub> solutions at 75 ± 5 °C for 20 min. The clean glass was rinsed with distilled water and then oven-dried (93 °C).

The clean substrates were loaded at a slant face down in a rack under argon.<sup>13</sup> A solution of 1 mL of (CH<sub>3</sub>O)<sub>3</sub>Si(CH<sub>2</sub>)<sub>3</sub>SH [or (CH<sub>3</sub>O)<sub>3</sub>Si(CH<sub>2</sub>)<sub>3</sub>NH<sub>2</sub> or (CH<sub>3</sub>O)<sub>3</sub>SiCH<sub>2</sub>CH(CH<sub>3</sub>)<sub>2</sub>] in 13 mL of toluene (pre-dried by refluxing over Na/K under argon) was injected through the serum cap and was refluxed for 4 h. Then the glass plates were rinsed with toluene, dried in a stream of argon and, unless immediately used, were stored in a desiccator.

**Preparation of gold films on microscope slides.** Gold–acetone colloidal solutions were prepared by the metal vapor SMAD (solvated metal atom dispersion) method, which has been described elsewhere.<sup>7,10,12</sup> Generally, about 100 mL of a gold–acetone solution was prepared with an Au loading of 0.05% by weight. The organically modified microscope slides were immersed in vials of Au–acetone colloidal solution for 5 s, 20 min, 1, 4, 12 or 24 h. The slides were rinsed with acetone, dried with an Ar stream and stored in a desiccator.

**Preparation of gold colloid deposits on different organically modified TEM grids.** The SiO<sub>x</sub> coated TEM grids were immersed in (CH<sub>3</sub>O)<sub>3</sub>Si(CH<sub>2</sub>)<sub>3</sub>X–methanol (v/v, 2 : 1) for 2.5 h, followed by extensive methanol rinses. The rinsing was accomplished by pipetting solvent across the grid surface, then using filter paper to absorb the solvent. These organically modified TEM grids were floated upside down on an Au–

† Non-SI unit employed: 1 Torr ≈ 133.3 Pa.

acetone colloid solution for 5 s, 1, 4 or 24 h. The glass dish containing the samples was filled with acetone vapor. Samples were rinsed with acetone and any excess of solvent was removed by touching the grid onto filter paper.

**Preparation of alkylamine-coated gold colloids.** The method was similar to the SMAD preparation of Au–acetone colloidal solution, that is,  $\approx 0.01\text{--}0.04$  g gold was vaporized and codeposited over 2 h with 100 mL acetone. After meltdown and inletting of argon into the reactor, a small amount of dodecylamine acetone solution was injected into the chamber (2 mL of a  $4.8 \times 10^{-3}$  M or 3 mL of a  $1.88 \times 10^{-2}$  M amine solution for a 25 : 1 or 1 : 1 molar ratio, respectively). Throughout the warming period, the colloid frozen matrix and dodecylamine were continuously stirred for 30–60 min. Finally, the brown solution was siphoned into a Schlenk tube under Ar.

The brown powder of dodecylamine-coated gold was obtained by evaporating acetone under vacuum, down to a pressure less than  $2 \times 10^{-3}$  Torr. This powder could be redissolved in acetone to give a brown solution.

## Methods

**AFM (atomic force microscopy).** The glass substrates ( $1.5 \times 3$  cm) were mounted on *ca.*  $2 \times 4$  cm steel holders with adhesive tabs. AFM experiments were conducted in air at *ca.* 295 K using a commercial AFM (SPM 30 from Wyco). The AFM was operated in constant force mode. A 100 mm long and rectangular cantilever with a spring force constant of  $0.37$  N  $\text{m}^{-1}$  and a  $\text{Si}_3\text{N}_4$  integrated pyramidal tip was used. Resolution was  $256 \times 256$  pixels. The AFM experiments were carried out on different parts of the surface to make sure that the observed structure was representative and reproducible.

**TEM (transmission electron microscopy).** TEM is a direct observation method concerning the morphology and interparticle spacing. Both the gold colloid sizes and the amine-coated gold colloid sizes were estimated from TEM studies. After the gold colloidal solution was agitated for 5 to 8 min in a sonicator, a drop of the suspension was transferred onto a carbon-coated copper grid as the sample holder. After evaporation of the solvent, the sample was ready for TEM study. TEM analysis of colloidal particles was performed on a Philips EM-201 instrument with an accelerating voltage of 100 kV. TEM images of alkylamine-coated Au particles were taken with a Philips CM-12 microscope operating at 100 kV.

**UV/VIS spectroscopy.** Absorption spectra were obtained using a SLM-Aminco Model 3000 Array (Milton Roy Co.) UV/VIS spectrophotometer.

**FT-IR.** The FT-IR spectrum of alkylamine-coated gold colloid was obtained on a Digilab Division 3240-SPC from Bio-Rad. The dried brown powder (dodecylamine-coated gold colloids) was ground with Nujol and then spread on a KBr window.

## Results and Discussion

### Atomic force microscopy studies of gold film growth on organically modified glass surfaces

**Glass substrate.** Shown in Fig. 1 is a  $1200 \text{ nm} \times 1200 \text{ nm}$  constant force AFM image of a clean glass surface. Marks due to mechanical polishing were observed running through the surface. Beside these marks, the surface was extremely flat and devoid of any defects. This roughness is attributed to the cutting, cleaning and handling procedure used by the manufacturer, but the surface was flat enough for our studies.

**Vapor-phase silane-modified glass substrates.** Thin films of alkoxysilanes on glass slides were prepared by exposing the

glass surfaces to the hot vapors of sufficiently volatile silanes in toluene for 1, 2, 4 or 7 h.

From the experiments, it was shown that the most uniform film was obtained with a reflux time of 4 h. The drying methods (oven drying or Ar flush) seemed to have no effect on the organic surface. Similar results were obtained with amine- and methyl-terminated surfaces.

There was no damage to organic films during AFM imaging. This result showed that the silanes were firmly bound to the glass surface.

**Comparison of Au colloid deposition on differently treated glass substrates.** There were noticeable differences in Au colloid deposition on the bare glass substrate in comparison to the organically modified surfaces. It appeared that on the unmodified glass surface there were no small Au particles, just large aggregates and these aggregates could be removed by the AFM tip, even at the lowest imaging forces. It is well-known that adhesion of Au to  $\text{SiO}_2$  is very weak, and thus, the particles readily aggregated into large islands of gold aggregates.

The Au colloids deposited on both  $(\text{CH}_3\text{O})_3\text{Si}(\text{CH}_2)_3\text{SH}$  (thiol)- and  $(\text{CH}_3\text{O})_3\text{Si}(\text{CH}_2)_3\text{NH}_2$  (amine)-treated glass substrates displayed no loss of Au during AFM investigation or even after adhesion testing with adhesive tape. We attribute this good adhesion to strong chemical interactions between Au and these two functional groups. The surface diffusion of Au colloids on the thiol and amine surfaces was substantially reduced compared with the untreated glass surface and so allowed the deposition and trapping of much smaller gold particles.<sup>14</sup> However, some larger aggregates were detected by AFM, in particular on the amine-terminated surface where a few flat-topped structures were imaged. Thus, gold particle diffusion on the surface was inhibited more by the thiol termination, which provides evidence for stronger particle–surface adhesion.<sup>15–18</sup>

**Evolution over time of gold films grown on thiol-terminated glass surfaces monitored by AFM.** It is of interest to determine the process by which the gold films grow. We know that colloidal particles of 6–9 nm make up the fundamental building blocks (Au crystallites) in the acetone liquid. However, these can weakly aggregate in solution before deposition on the

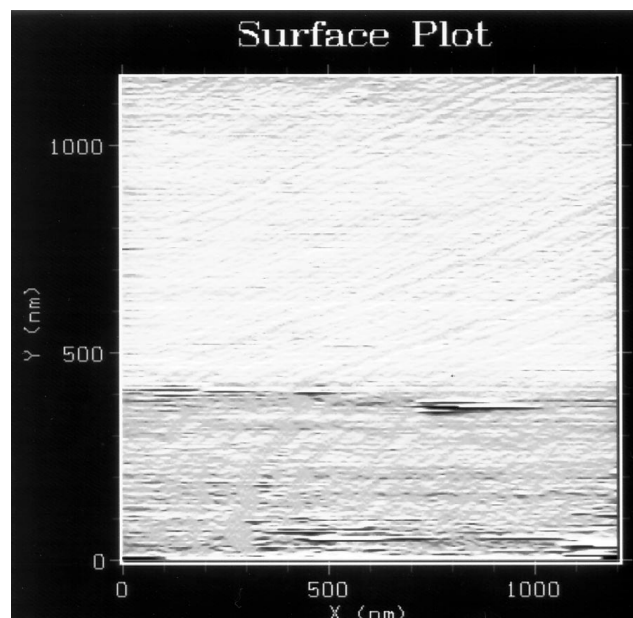


**Fig. 1**  $1200 \text{ nm} \times 1200 \text{ nm}$  constant force AFM image of a clean glass surface. The glass was cleaned in 30%  $\text{H}_2\text{O}_2$  : 98%  $\text{H}_2\text{SO}_4$  (v/v, 1 : 4) solution at  $75 \pm 5^\circ\text{C}$  for 20 min, then rinsed with distilled water and dried in an oven ( $93^\circ\text{C}$ )

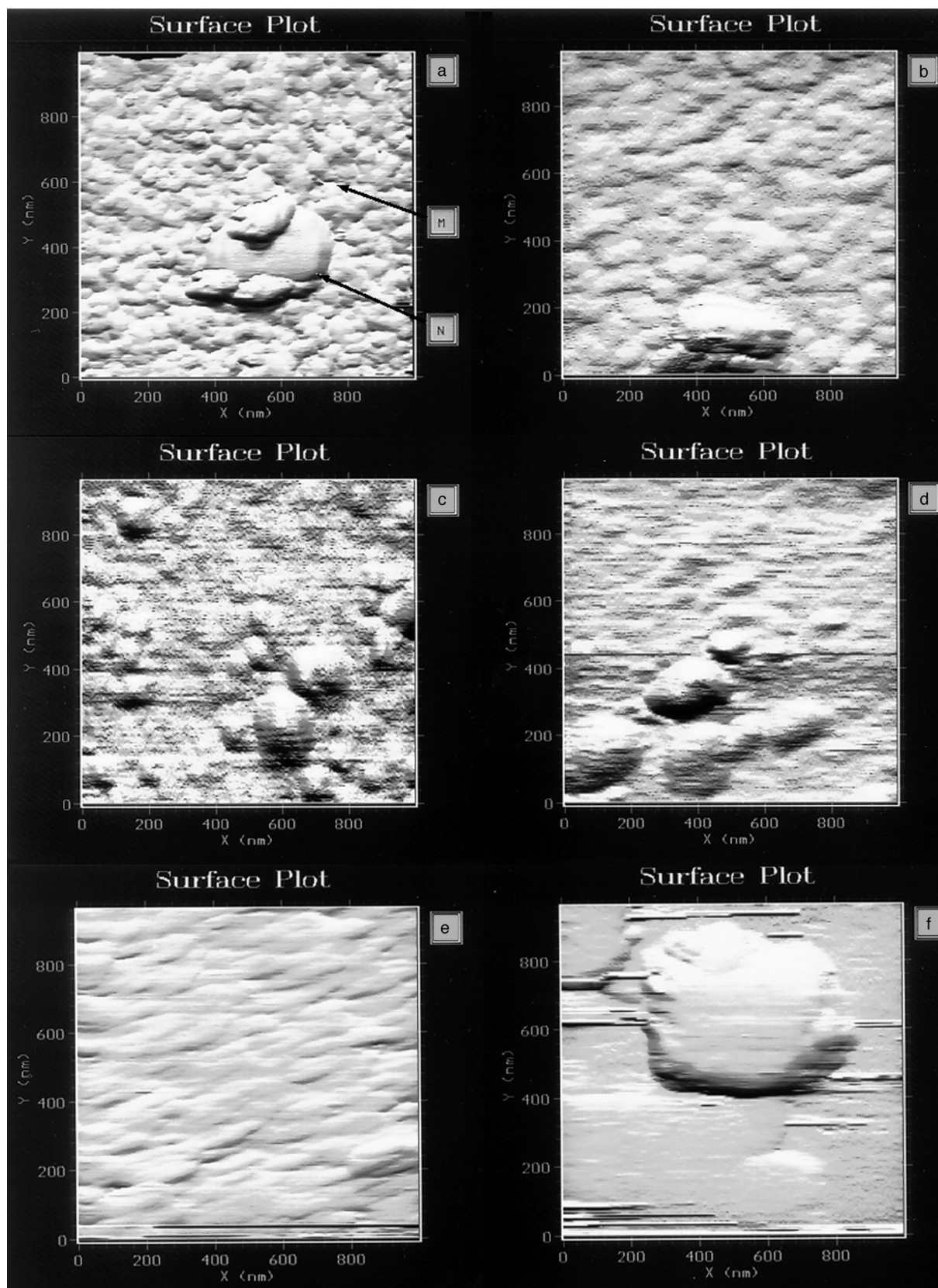


**Fig. 2** 1000 nm  $\times$  1000 nm constant force AFM images of Au colloids deposited on  $(\text{CH}_3\text{O})_3\text{Si}(\text{CH}_2)_3\text{SH}$ -modified glass surfaces with different deposition times: (a) 5 s (an organic particle is shown at M, size: 20 nm; an Au cluster is shown at N, size: 320 nm); (b) 20 min; (c) 1 h; (d) 4 h; (e) 12 h; (f) 24 h

substrate, or they can deposit and then migrate on the surface (gold self-diffusion) and thereby grow larger islands. This type of diffusion would depend on the strength of interaction between the fundamental gold particles and the substrate. A weak Au-substrate interaction would allow facile self-diffusion, whereas a strong Au-substrate interaction would discourage self-diffusion and island growth, but instead would

enable a more two-dimensional film growth.

Another growth mechanism can also be envisioned. If gold particles form aggregates before deposition on the substrate, and if the Au-substrate interaction is stronger than the Au particle-Au particle interaction, then the aggregates may break up and the Au particles spread out more evenly on the surface.

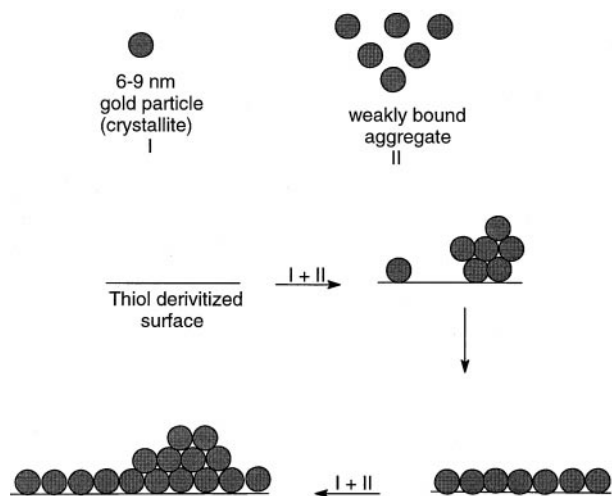


**Fig. 3** Process of film growth from Au-acetone colloids on thiol-terminated surfaces

According to AFM [Fig. 2(a)–(f)] at short deposition times (5 s), individual gold particles and a few aggregates adsorbed on the thiol-terminated surface. After 1 h of deposition a thin gold film had been produced, indicating that gold particle adhesion was good and gold self-diffusion was limited. It also indicated that aggregates detected after shorter contact times had dispersed. After 4 h, however, the rate of gold particle adsorption and gold products self-diffusion began to be important. Thus, as Au particles began to form multilayers, the Au particles–Au surface interaction was weak enough that the Au particles could diffuse and in this way stable aggregates or islands were formed. Indeed, with further deposition times flat-topped large islands formed, and this indicates that self-diffusion and particle dispersion were about equal. Fig. 3 illustrates pictorially this sequence and Table 1 gives further details.

### Transmission electron microscopy studies

**Embryonic stages of island and film growth on thiol-, amine- and methyl-terminated surfaces of TEM specimens.** Although AFM was helpful in elucidating general features of film growth, we turned to TEM for more information about the beginning stages of deposition, island formation and film growth. For these studies, silica-coated TEM grids were employed; these were treated with the functionalized silanes in methanol, followed by methanol rinse (see Experimental) and then soaked in the Au-acetone colloidal solution for varying times.

Fig. 4–6 illustrate typical and reproducible TEM photographs of gold particles/aggregates obtained at different soak times with thiol-, amine- and methyl-terminated grids. Careful inspection reveals a number of interesting features about the mode of deposition and dispersion on the thiol-terminated surface (Fig. 4). After 5 min exposure to the colloid solution, the grid was sparsely covered mainly with gold particle aggregates. However, after 1 h of soaking, the aggregates had disappeared and individual spherical particles in the 5–10 nm range dominated. This finding mimics that found in the previously discussed AFM studies, where apparently the colloid solution deposits aggregates of the individual particles, but then these aggregates mainly come apart and disperse on the surface (Au particle–surface adhesion is greater than Au particle–Au particle adhesion in the initially deposited aggregates), although some coalescence to form larger spheres is also evident. After 4 h, further coalescence has occurred and after 24 h this continued coalescence allows formation of a network structure that is tending toward a continuous film.

**Table 1** Comparison of different times for gold colloid deposition on thiol-modified substrates<sup>a</sup>

Time	Comments
5 s	A few large aggregates as well as individual particles are deposited.
20 min	Particles are smaller than those observed after 5 s deposition, but more uniform.
1 h	The surface is flatter and smoother, and more large particles appear on the surface. Small particles are almost absent.
4 h	Large particles (200–300 nm) increase on the flat surface and the border of the particles is clear.
12 h	On a flat surface, the border of particles disappear. A multilayer film forms.
24 h	Multilayer of gold film is present. Aggregates coalesce to form big particles with flat tops. [Fig. 8(f)]

<sup>a</sup>Goss and co-workers discuss typical gold particle morphologies.<sup>19</sup>

Similar results were obtained on amine-terminated substrates (Fig. 5). First, aggregates were deposited, which then dispersed as individual gold particles. However, on the amine surface there was less evidence of coalescence and after 24 h there still was no network formation. These results suggest that the initial weakly bound aggregates do disperse, but then continued surface migration is slightly less favoured so that particle coalescence is slower. Apparently the Au particle surface diffusion rate is lower on the amine surface than the thiol surface, indicating a somewhat stronger interaction. Interestingly, this behaviour tended to inhibit network/film formation.

On the methyl-terminated surface, we expected rapid surface diffusion of particles and aggregates, since the  $-\text{CH}_3$ –gold interaction should be relatively weak. Indeed, Fig. 6 shows that particles and aggregates adsorbed and that diffusion and growth occurred relatively rapidly. Interestingly, however, over time the surface concentration of gold did not increase and actually appears to decrease. These results suggest that particles and aggregates that adsorbed moved easily, coalesced into larger particles and that some of these larger particles then were lost/removed from the surface. It seems as though this nonpolar surface induced particle coalescence and the loss of these large particles, thus behaving as a catalyst for growth/coalescence. Particle–particle interaction is much stronger than particle–surface interaction and this leads to larger particles, loss of some of these, and a low overall coverage even after long term exposure to the Au-acetone colloid solution.

**Treatment of the Au-acetone colloid with an alkylamine.** The preceding results indicated that the gold colloid particles were very likely weakly aggregating in solution before deposition. This aggregation is not a coalescence and so the individual Au particles (crystallites) remained in the 6–9 nm range, most about 7 nm. Therefore, we decided to trap the crystallites during different stages of the atom  $\rightarrow$  7 nm crystallite growth process. In order to do this a long-chain alkylamine was added to cap the crystallite and impede the aggregation process. Dodecylamine was chosen and we then expected to isolate individual crystallites separated by 1–2 nm due to the length of the alkyl chain.

Earlier work had shown that the Au atom  $\rightarrow$  crystallite growth occurred during the warm-up of the Au atom–acetone frozen matrix.<sup>9,10,12</sup> Therefore, in the present study, the acetone matrix was allowed to melt ( $-95^\circ\text{C}$ ) and then varying amounts of dodecylamine were added by syringe under argon, followed by stirring and warming to room temperature over 1 h. The resultant solution was red-brown and by acetone evaporation a brown powder was obtained, which

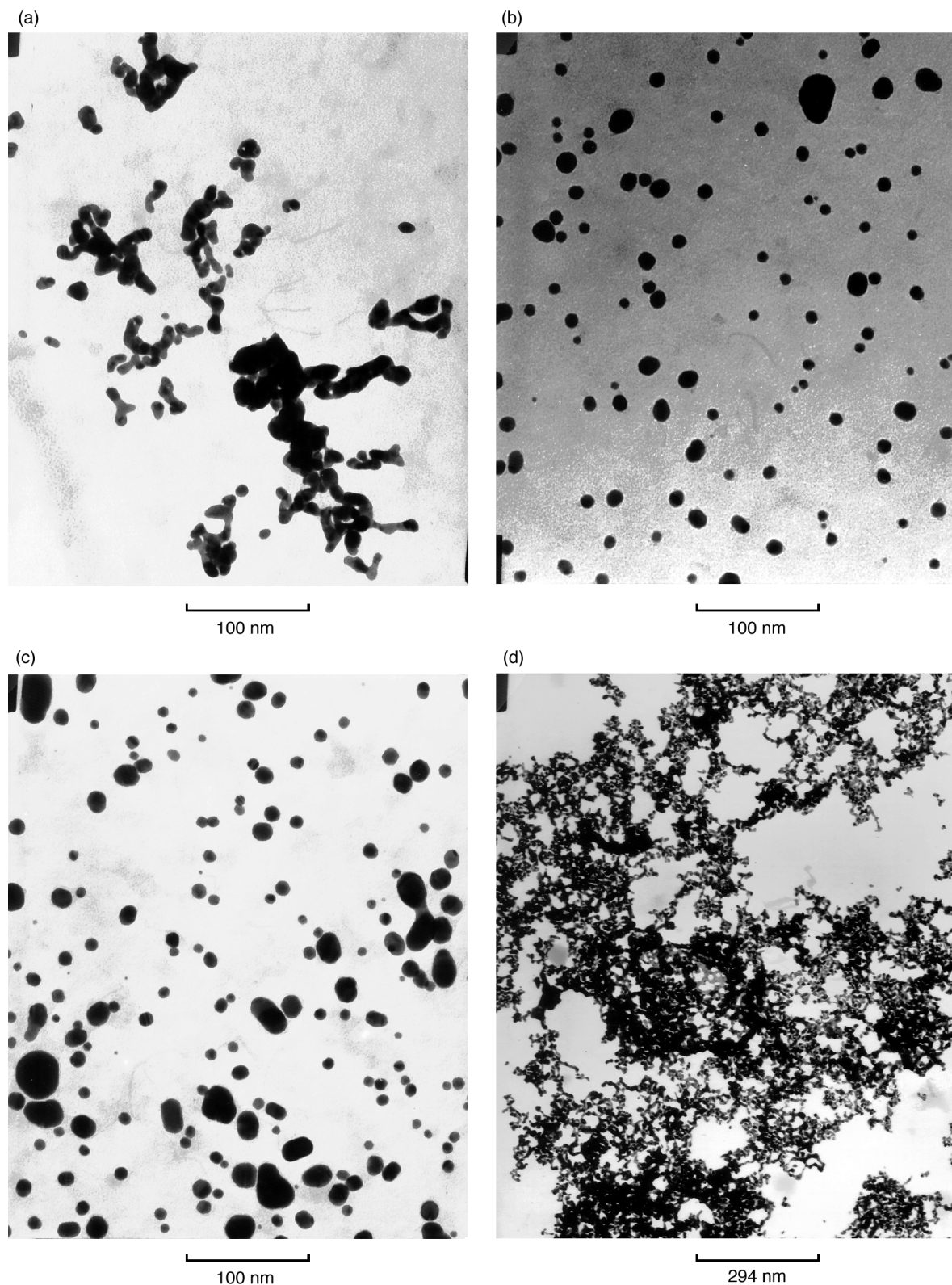


**Fig. 4** TEM micrographs of  $(\text{CH}_3\text{O})_3\text{Si}(\text{CH}_2)_3\text{SH}$ -coated TEM grids derivatized in 7 nm Au colloids for (a) 5 min (magnification  $\times 198\,300$ ); (b) 1 h ( $\times 198\,000$ ); (c) 4 h ( $\times 198\,300$ ); (d) 24 h ( $\times 68\,000$ )

could readily be redissolved in acetone.

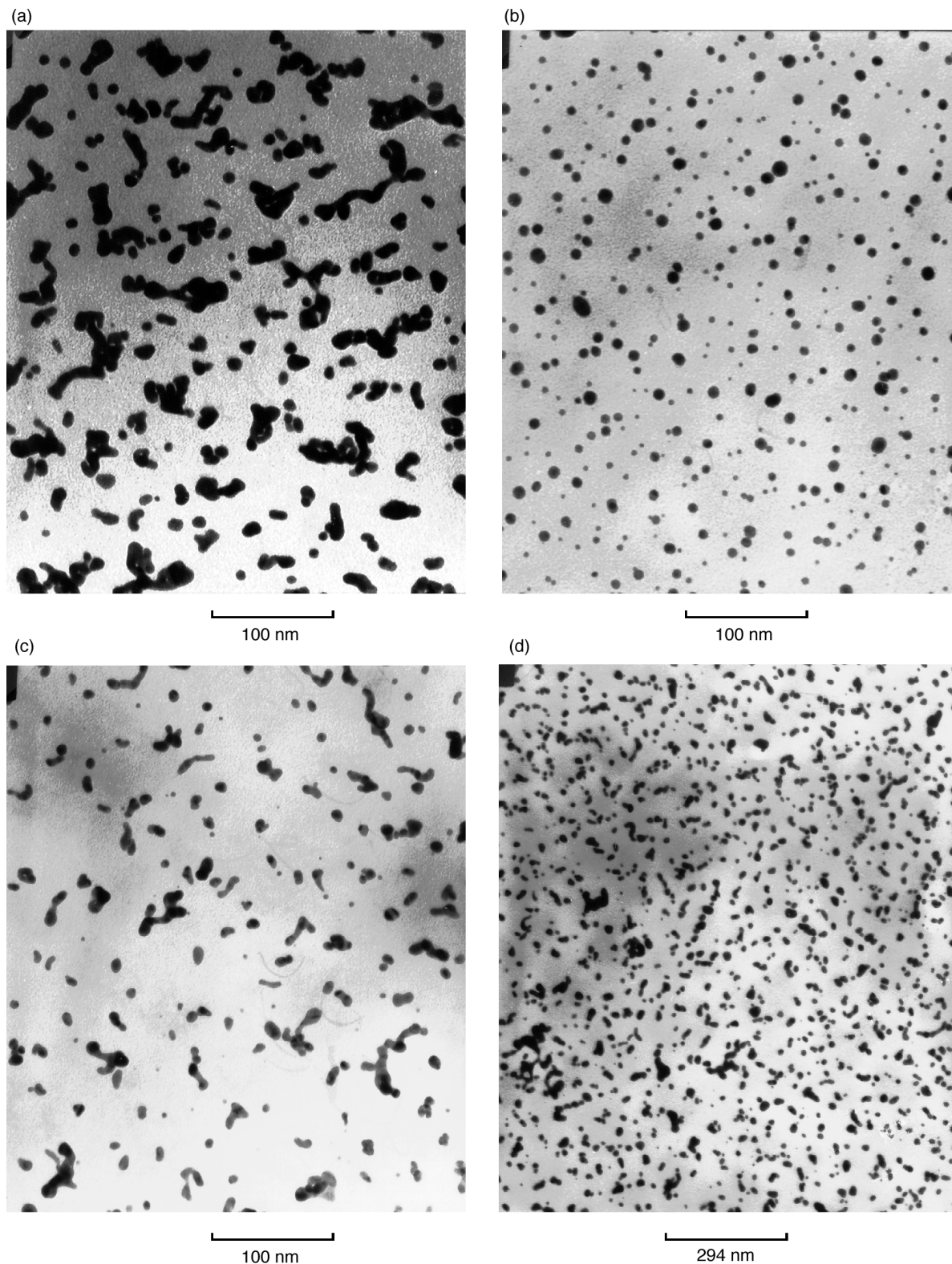
By dilution and placing a drop of the Au–dodecylamine–acetone solution on TEM grids followed by acetone evaporation, good quality TEM prints were obtained.

Fig. 7 shows the Au–dodecylamine particles from a solution containing a molar ratio of amine-to-gold of 1 : 25 (1 amine molecule to 25 gold atoms). A dense array of 2–5 nm gold crystallites was observed with most particles clearly separated by the amine coating. Furthermore, only a single layer was formed (two dimensional) and no evidence for coalescence to

larger crystallites is seen.

When much larger amounts of amine were used, such as a molar ratio of amine-to-gold of 1 : 1, even smaller crystallites were isolated ( $\approx 3$  nm) and their interspatial separation was less uniform (Fig. 8).

We also obtained UV/VIS spectra on Au–dodecylamine–acetone solutions (Fig. 9) (molar ratio 25 : 1 gold : amine). A  $\lambda_{\text{max}}$  of 531 nm was observed, which is blue-shifted about 18 nm from the pure Au–acetone colloid where  $\lambda_{\text{max}} = 549$  nm. Since the TEM results indicate that the crystallites are about 3



**Fig. 5** TEM micrographs of  $(\text{CH}_3\text{O})_3\text{Si}(\text{CH}_2)_3\text{NH}_2$ -coated TEM grids derivatized in 7 nm Au colloids for (a) 5 min (magnification  $\times 198\,300$ ); (b) 1 h ( $\times 198\,300$ ); (c) 4 h ( $\times 198\,300$ ); (d) 24 h ( $\times 68\,000$ )

nm in the Au-amine-acetone solutions, but are about 7 nm in the Au-acetone solution, such a blue shift is reasonable. However, the presence of the adsorbed amine may also play a role and it is difficult to separate the two effects of size *vs.* different adsorbate.

The dry Au-amine powder (molar ratio 25:1) was dispersed in mineral oil and an IR spectrum obtained, which exhibited both  $\nu_{\text{N-H}}$  and  $\nu_{\text{C=O}}$  bands (Fig. 10). These results

indicate that acetone and probably the amine remain adsorbed on the gold particles. Even evacuation of the Au-amine sample to  $1 \times 10^{-3}$  Torr for 1 h failed to remove these strongly chemisorbed species. It is interesting that this sample, after evacuation, could readily be redissolved in acetone. Such behaviour was not observed when only acetone (no amine) was present. Therefore, the amine must also be present in a chemisorbed state.

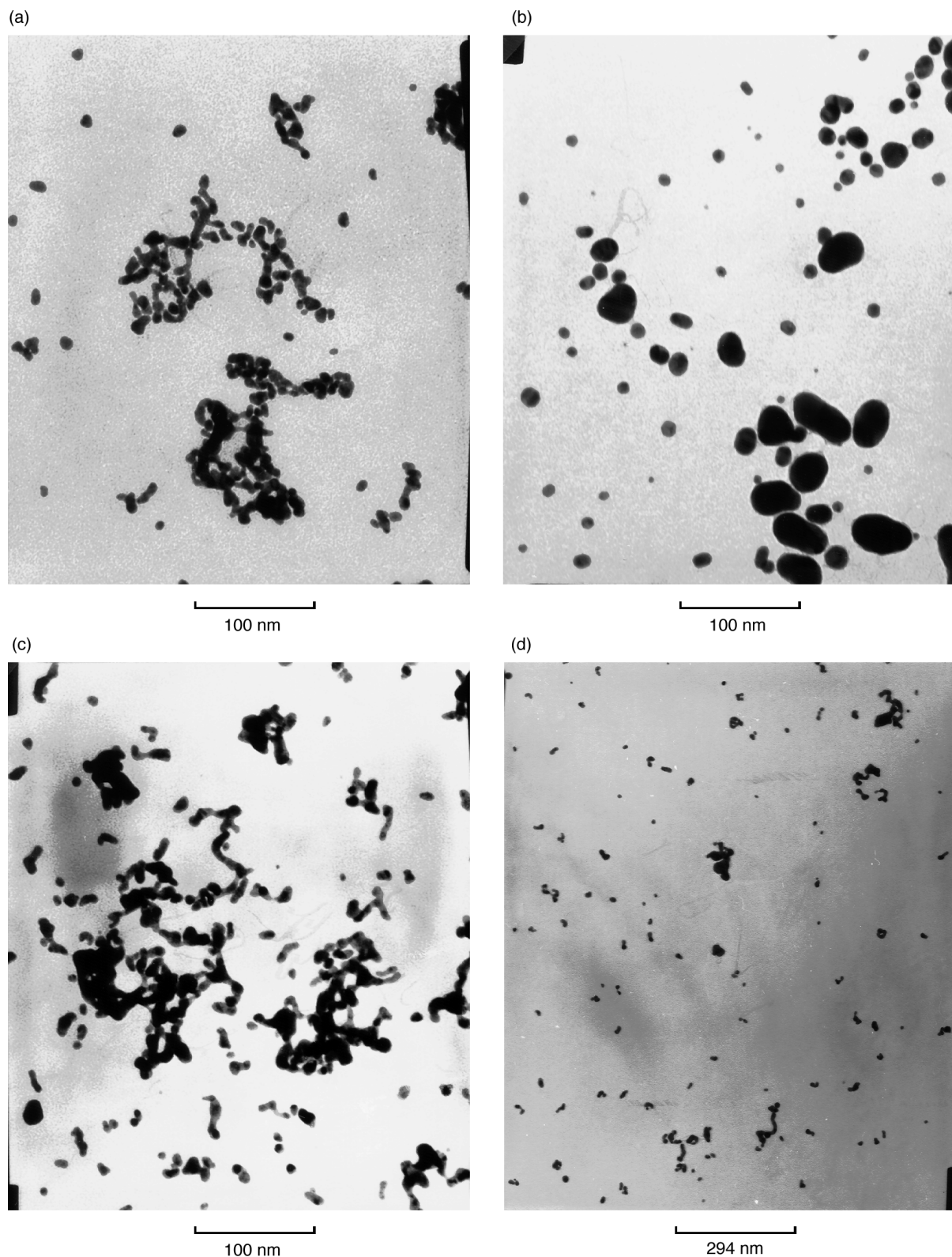


**Fig. 6** TEM micrographs of  $(\text{CH}_3\text{O})_3\text{SiCH}_2\text{CH}(\text{CH}_3)_2$ -coated TEM grids derivatized in 7 nm Au colloids for (a) 5 min (magnification  $\times 198\,300$ ); (b) 1 h ( $\times 198\,300$ ); (c) 4 h ( $\times 198\,300$ ); (d) 24 h ( $\times 68\,000$ )

## Conclusions

The results of this study lead to the following conclusions:

(1) They reaffirm that Au vapor–acetone codepositions lead to colloidal solutions consisting of Au crystallites of about 7 nm in diameter and that these colloidal solutions are made up of solvated individual crystallites, as well as weakly agglomerated clusters.

(2) When these particles (aggregates as well as individual crystallites) adsorb on organically modified surfaces:

(a) On thiol-derivitized surfaces gold particles and aggregates randomly adsorbed rather strongly and eventually a mesh-like film formed, (Fig. 3).

(b) On amine-derivitized surfaces strong adsorption also occurred, leading to short chains with more even interparticle spacing.

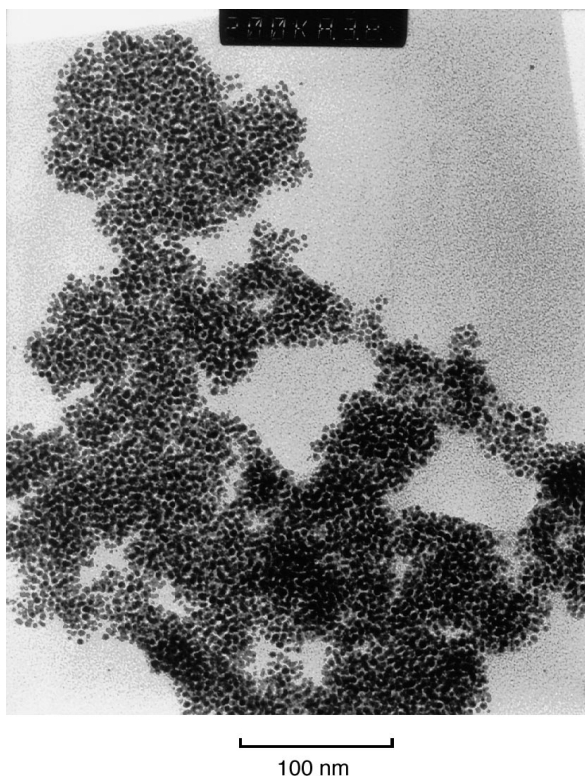


**Fig. 7** TEM micrograph of dodecylamine-coated gold colloids during SMAD reaction with a 25:1 molar ratio of gold-to-dodecylamine (magnification  $\times 200\,000$ )

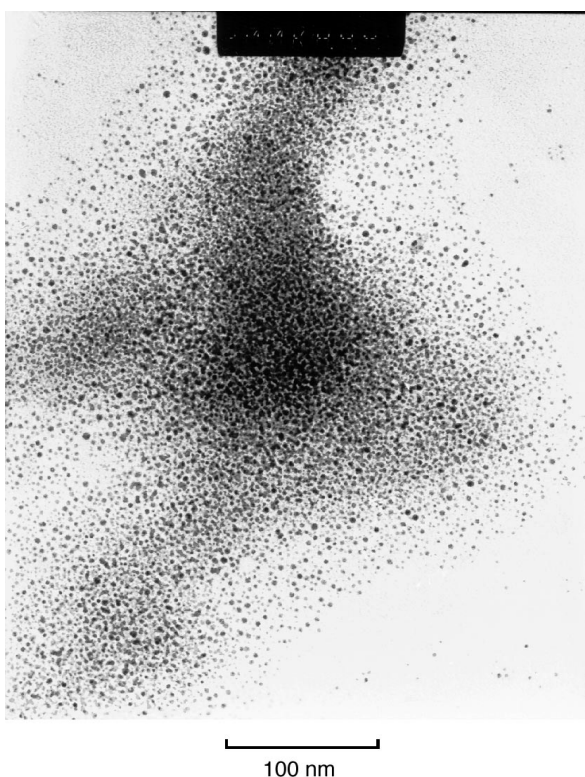


**Fig. 8** TEM micrograph of dodecylamine-coated gold colloids during SMAD reaction with a 1:1 molar ratio of gold-to-dodecylamine (magnification  $\times 200\,000$ )

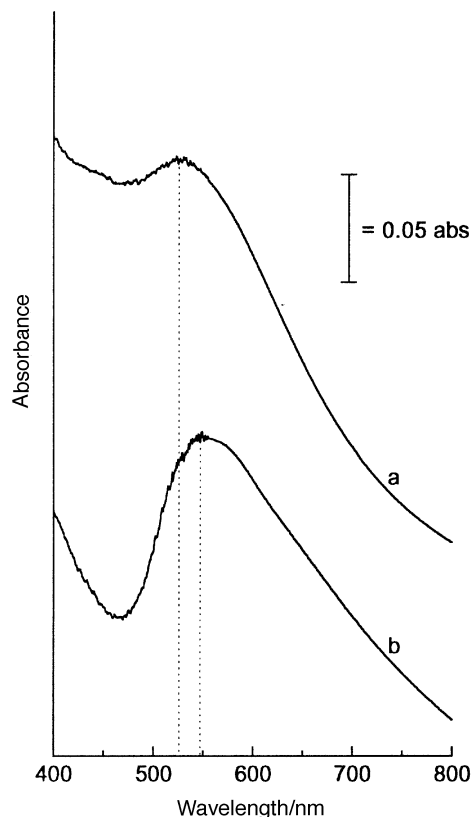


**Fig. 9** UV/VIS spectra of (a)  $\text{Au-CH}_3(\text{CH}_2)_{11}\text{NH}_2$  (molar ratio is 25:1) acetone colloidal solution (concentration is  $2.4 \times 10^{-4}$  M,  $\lambda_{\text{max}} = 531$  nm); (b) pure Au-acetone colloidal solution (concentration is  $4.9 \times 10^{-4}$  M,  $\lambda_{\text{max}} = 549$  nm)

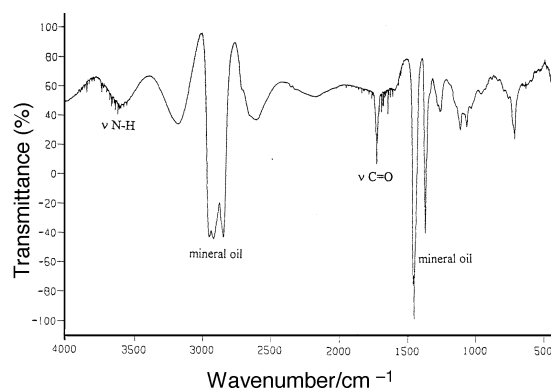


**Fig. 10** IR spectrum of dry  $\text{Au-CH}_3(\text{CH}_2)_{11}\text{NH}_2$  (molar ratio is 25:1) powder in mineral oil. Peaks due to mineral oil: 2952, 2924,  $2858\text{ cm}^{-1}$ . Peaks at 3608,  $3192\text{ cm}^{-1}$  are due to  $\nu_{\text{N-H}}$  (amine); the peak at  $1734\text{ cm}^{-1}$  is due to  $\nu_{\text{C=O}}$  (acetone)

(c) On methyl-derivitized surfaces adsorption was much weaker leading to more particle diffusion, coalescence and then facile loss from the surface by solvent action.

(3) We have succeeded in trapping with a long-chain alkylamine even smaller Au crystallites of 2–5 nm diameter. This was accomplished by adding the amine at low temperature, thereby interrupting the atom  $\rightarrow$  crystallite growth before the 7 nm size is reached (Fig. 11). This shows that the atom  $\rightarrow$  crystallite growth occurs in the cold liquid acetone over time and in the absence of amine, growth continues until crystallites of about 7 nm are reached. Growth then stops due to a combination of lower particle mobility combined with solva-

Au atoms in cold, melting acetone

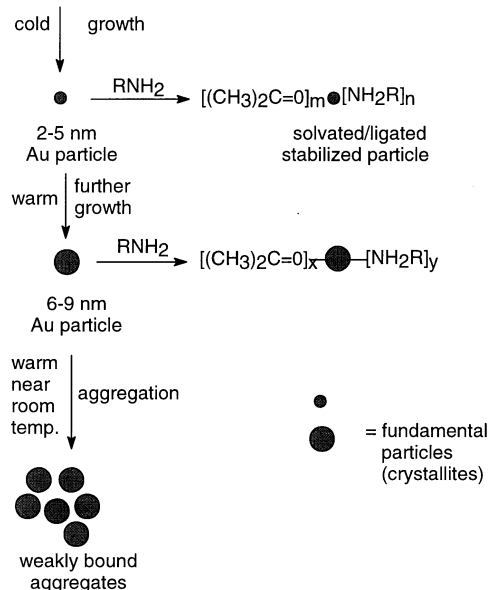


Fig. 11 Gold atom migration and growth in cold acetone. Trapping of small clusters with dodecylamine

tion.<sup>7</sup> The 2–5 nm crystallites that are trapped by amine are stable toward further growth and possess chemisorbed amine and acetone moieties. These trapped crystallites have molecular properties, are stable and readily redissolve. In fact, solutions possess different colours depending on the solvent, there is good solubility in 2-propanol (dark blue), pyridine (brown) and THF (blue), moderate solubility in water (purple) and poor solubility in toluene and pentane (black precipitates). The particles showed good solubility in 2-propanol, pyridine and THF, moderate solubility in water and poor solubility in toluene and pentane.

There are several points of interest about these results. First, this method of deposition of gold particles leads to thin films with good adhesion and these could be useful for further spectroscopic investigations. Second, the mechanism of gold deposition is of interest and could be applicable to other assembly processes. Finally, the small alkylamine-coated gold crystallites of 2–3 nm are of intrinsic interest in their own right. These materials behave like simple chemical compounds; they can be precipitated and redissolved without any apparent change in properties. They are uniform, noninteracting small gold particles in solution.

## Acknowledgements

The support of the National Science Foundation is acknowledged with gratitude. We also thank Drs. Avelina Q. Paulsen, Dajie Zhang (Kansas State University), and Isabelle Lagadic (Oklahoma State University) for assistance with AFM and TEM investigations.

## References

- 1 K. C. Grabar, R. G. Freeman, M. B. Hommer and M. J. Natan, *Anal. Chem.*, 1995, **67**, 735.
- 2 R. G. Freeman, K. C. Grabar, K. J. Allison, R. M. Bright, J. A. Davis, A. P. Guthrie, M. B. Hommer, M. A. Jackson, P. C. Smith, D. G. Walter and M. J. Natan, *Science*, 1995, **267**, 1629.
- 3 M. Giersig and P. Mulvaney, *Langmuir*, 1993, **9**, 3408.
- 4 A. Doron, E. Katz and I. Willner, *Langmuir*, 1995, **11**, 1313.
- 5 K. C. Grabar, K. J. Allison, B. E. Baker, R. M. Bright, K. R. Brown, R. G. Freeman, A. P. Fox, C. D. Keating, M. D. Musick and M. J. Natan, *Langmuir*, 1996, **12**, 2353.
- 6 K. C. Grabar, P. C. Smith, M. D. Musick, J. A. Davis, D. G. Walter, M. A. Jackson, A. P. Guthrie and M. J. Natan, *J. Am. Chem. Soc.*, 1996, **118**, 1148.
- 7 K. J. Klabunde, G. Youngers, E. J. Zuckerman, B. J. Tan, S. Antrim and P. M. A. Sherwood, *Eur. J. Solid State Inorg. Chem.*, 1992, **29**, 227.
- 8 (a) G. Cardenas-Trivino, K. J. Klabunde and B. Dale, *SPIE: Modeling of Optical Thin Films*, 1987, **821**, 206. (b) B. Rabinovich, R. H. Horner, K. J. Klabunde and P. Hooker, *Metalsmith*, 1994, **14**, 41.
- 9 B. J. Tan, P. M. A. Sherwood and K. J. Klabunde, *Langmuir*, 1990, **6**, 105.
- 10 S.-T. Lin, M. T. Franklin and K. J. Klabunde, *Langmuir*, 1986, **2**, 259.
- 11 G. Cardenas-Trivino, K. J. Klabunde and E. B. Dale, *Langmuir*, 1987, **3**, 986.
- 12 (a) M. T. Franklin and K. J. Klabunde, in *High Energy Processes in Organometallic Chemistry*, ed. K. Suslick, ACS Symposium Series 333, American Chemical Society, Washington, DC, 1987, pp. 247–259. (b) K. J. Klabunde and G. Cardenas in *Active Metals. Preparation, Characterization, Application*, ed. A. Furstner, VCH, Weinheim, 1996, pp. 237–278.
- 13 I. Haller, *J. Am. Chem. Soc.*, 1978, **100**, 8050.
- 14 D. J. Dunaway and R. L. McCarley, *Langmuir*, 1994, **10**, 3598.
- 15 C. D. Bain, J. Evall and G. M. Whitesides, *J. Am. Chem. Soc.*, 1989, **111**, 7155.
- 16 G. Horanyi and S. B. Orlov, *J. Electroanal. Chem.*, 1991, **309**, 239.
- 17 C. A. Widrig, C. Chung and M. D. Porter, *J. Electroanal. Chem.*, 1991, **310**, 335.
- 18 C. Xu, L. Sun, L. J. Kepley, R. M. Crooks and A. M. Ricco, *Anal. Chem.*, 1993, **65**, 2102.
- 19 C. A. Goss, J. C. Brumfield, E. A. Irene and R. W. Murray, *Langmuir*, 1993, **9**, 2986.

Received in Montpellier, France, 6th November 1997;  
Paper 7/09248B